When Stability Becomes Fragility: Phase Transitions in Financial Markets

Tomás Basaure Larraín*

December 2025

Abstract

Financial crises frequently emerge after prolonged periods of apparent stability, when volatility is low and standard risk metrics signal safety. This paper provides evidence that the mapping from market structure to systemic tail risk is regime-dependent, exhibiting characteristics of a phase transition. A new state variable, Accumulated Spectral Fragility (ASF), is introduced to measure the persistent low-dimensionality of correlation structures over medium horizons. Using global multi-asset data from 1990–2024, a threshold regression framework identifies a critical connectivity level (average correlation $\tau \approx 0.14$) that partitions the sample into two distinct regimes. Below the threshold, structural fragility amplifies future tail risk through contagion dynamics. Above the threshold, the relationship inverts: systemic episodes are instead preceded by a loss of coupling, consistent with disintegration dynamics in hyper-connected markets. The estimated regime-specific coefficients differ significantly ($p < 0.01$), and results are robust to extensive specification checks including Monte

*Pontificia Universidad Católica de Chile. Email: tbasaure@uc.cl. The author thanks [acknowledgments]. Replication materials available at [URL]. Online Appendix available at [URL].

Carlo simulations, placebo tests, subsample analysis, and out-of-sample forecasting. These findings provide a structural resolution to the volatility paradox and suggest that macroprudential monitoring in modern, tightly coupled markets requires tracking structural state variables rather than volatility alone.

Keywords: systemic risk; endogenous fragility; phase transition; financial networks; spectral entropy; threshold regression

JEL Codes: G01, G12, C24, C58

1 Introduction

Financial crises tend to arrive when they are least expected. Some of the most severe systemic episodes of the past four decades—from the 1987 stock market crash to the 2008 Global Financial Crisis to the 2020 COVID-induced market turmoil—occurred after prolonged periods of tranquility, when realized and implied volatility were subdued and conventional risk measures suggested safety (Reinhart and Rogoff, 2009; Danielsson et al., 2018). This empirical regularity is difficult to reconcile with linear frameworks in which risk rises smoothly with volatility. It is, however, consistent with a broadly Minskyan view of endogenous fragility: stability alters behavior, behavior alters balance sheets and market structure, and the resulting system can become vulnerable in ways not visible in short-horizon price variability (Minsky, 1992; Geanakoplos, 2010).

This paper argues that the key object is not volatility per se, but the structural state of market connectivity. The central claim is that the mapping from connectivity to systemic risk is not monotone. Instead, financial markets exhibit a phase transition in the way structure translates into tail outcomes. Below a critical connectivity threshold, additional coupling increases the scope for cascades: fragility is "contagious" in the standard sense (Allen and Gale, 2000; Gai and Kapadia, 2010). Above that threshold, the market behaves as an over-connected cluster whose short-run stability depends on maintaining cohesion. In this regime, crises are preceded not by further increases in coupling, but by the breakdown of coupling—a disintegration of the structural substrate that supports liquidity provision and coordinated pricing.

The intuition can be grasped through an analogy with physical systems. Consider a network of interconnected nodes. At low connectivity, the network consists of fragmented clusters; adding links creates pathways for disturbances to spread. This is

the classic contagion story: connectivity breeds vulnerability. But once the network becomes sufficiently dense—once a "giant component" spans the system—further connectivity changes the nature of risk. The system now behaves as a unified entity, and stability depends on maintaining that unity. The dangerous moment is no longer when links form, but when they break. A sudden loss of synchronization in a hyper-connected market triggers disintegration dynamics: hedges fail, liquidity evaporates, and fire sales cascade not because of excessive coupling, but because of its sudden absence.

This paper makes four main contributions. First, evidence is provided for a critical coupling threshold in financial markets at which the effect of structural fragility on future tail risk inverts sign. This formalizes a structural transition from "contagion" dynamics to "disintegration" dynamics in financial risk propagation. The estimated threshold ($\hat{\tau} \approx 0.14$ in terms of average correlation) is remarkably stable across specifications and time periods, suggesting it reflects a fundamental property of market microstructure rather than a sample artifact.

Second, Accumulated Spectral Fragility (ASF) is introduced as a state variable that captures the time-integrated persistence of low-dimensional market structure. Unlike static, contemporaneous risk indicators such as the Absorption Ratio (Kritzman et al., 2011), CoVaR (Adrian and Brunnermeier, 2016), and SRISK (Brownlees and Engle, 2017), ASF exhibits memory: it accumulates during periods of low entropy and decays slowly. This property allows ASF to detect the buildup of structural fragility even when short-run volatility remains subdued—precisely the conditions that precede major crises.

Third, a rigorous econometric validation is conducted using threshold regression methods (Hansen, 2000), HAC-robust inference (Newey and West, 1987), bootstrap confidence intervals, Monte Carlo simulations, temporal placebo tests, and surrogate

data falsification (Theiler et al., 1992). The nonlinearity is genuine: it survives randomization of temporal structure and appears in simulated data with known properties.

Fourth, the findings are shown to generalize across asset classes, time periods, and alternative risk measures, with implications for macroprudential policy (Hanson et al., 2011; Borio, 2014). A regime-conditional investment strategy demonstrates the economic significance of the phase transition: by adjusting exposure based on regime identification, one achieves meaningful improvements in risk-adjusted returns, suggesting the structural information in ASF is not fully priced.

The empirical analysis utilizes a panel of 47 major ETFs spanning U.S. sectors, international markets, fixed income, commodities, and alternatives from 2007–2024, with a longer out-of-sample global asset dataset (38 assets, 1990–2024) for validation. A nonlinear threshold regression is employed to estimate the critical connectivity level τ and the regime-specific effects of fragility on crash risk. The results reveal a highly significant split between two regimes. When average market correlation is below $\tau \approx 0.14$, higher fragility amplifies future tail risk ($\theta_L > 0$, with t-statistic 6.60). When connectivity exceeds τ, the coefficient on fragility flips sign ($\theta_H < 0$, with t-statistic -2.10): risk emerges from the loss of coupling rather than its formation. The Wald test for regime difference is highly significant ($\chi^2 = 42.7$, $p < 0.001$).

These findings help reconcile the volatility paradox: why severe crashes can erupt out of seemingly calm, highly correlated markets (Brunnermeier and Sannikov, 2014; Danielsson et al., 2012). The resolution lies in recognizing that broadly connected markets render volatility an insufficient statistic for systemic risk. At high connectivity, the dangerous moment is not when volatility is high, but when the system is hyper-connected yet suddenly loses synchronization. Volatility-based rules that relax leverage constraints when VIX is low may be precisely wrong in the Disintegration

regime.

The remainder of the paper proceeds as follows. Section 2 reviews related literature. Section 3 presents the theoretical framework with formal propositions and proofs. Section 4 describes data and methodology. Section 5 presents core empirical results. Section 6 summarizes robustness checks. Section 7 analyzes the hysteresis dynamics of systemic fragility. Section 8 validates the economic significance through a trading strategy. Section 9 discusses policy implications. Section 10 concludes.

2 Related Literature

This paper connects several strands of literature in financial economics, macroeconomics, and network science.

2.1 Endogenous Fragility and the Volatility Paradox

The paper relates to a long tradition emphasizing that financial stability can be self-undermining. Minsky (1992) proposed that tranquil periods induce risk-taking and balance-sheet fragility that eventually makes the system vulnerable to nonlinear adjustments. During quiet times, successful speculation encourages more aggressive positions; margins decline, leverage rises, and the distance to distress shrinks even as measured volatility falls. This "financial instability hypothesis" implies that stability itself is destabilizing.

Modern macro-finance models formalize related mechanisms. Brunnermeier and Sannikov (2014) develop a continuous-time model in which financial intermediaries amplify shocks through leverage dynamics. When measured risk is low, intermediaries lever up, generating a volatility paradox: the system becomes most fragile precisely when volatility is low. Adrian and Shin (2010, 2014) document procyclical leverage in

the financial sector, showing that risk-taking expands when Value-at-Risk constraints relax. Geanakoplos (2010) analyzes leverage cycles and their role in amplifying asset price volatility.

Danielsson et al. (2012) distinguish between perceived risk—lowest at the peak of a boom—and actual risk—highest precisely then due to endogenous leverage. Their framework suggests that any volatility-based risk measure will be misleading near cycle peaks. Danielsson et al. (2018) provide historical evidence that low volatility periods reliably precede financial crises. Schularick and Taylor (2012) document that credit booms predict financial crises across 140 years of data in 14 countries.

The present study contributes to this literature by providing empirical evidence that market structure exhibits regime-dependent links to subsequent tail risk. The phase transition framework formalizes the Minskyan intuition: fragility can accumulate silently during stable periods, and the mapping from fragility to realized risk depends on the structural state of the market.

2.2 Network Propagation and Systemic Risk

Financial markets can be viewed as networks where risk propagation depends on topology and link weights. Allen and Gale (2000) develop a model of financial contagion where the pattern of interbank claims determines systemic vulnerability. Acemoglu et al. (2015) analyze how network structure affects the resilience of financial systems, showing that connectivity can be a double-edged sword: it disperses small shocks but amplifies large ones.

Gai and Kapadia (2010) show that highly connected networks can be "robust-yet-fragile": resilient to most shocks but catastrophically vulnerable to rare large disturbances. Battiston et al. (2012) demonstrate that connectivity can initially re-

duce risk through diversification but eventually amplify it when the network becomes too dense. Elliott et al. (2014) model financial networks with cross-holdings and show how integration can create systemic fragility. Glasserman and Young (2016) provide a comprehensive review of contagion mechanisms in financial networks.

The concept of percolation from statistical physics is also relevant (Haldane and May, 2011; May et al., 2008). Below a critical connectivity, the network consists of fragmented clusters; above it, a giant component spans the system. This phase transition has been proposed as a model for financial contagion, but the relationship between network structure and systemic risk in actual financial markets has received limited empirical attention. The present paper provides evidence that financial markets exhibit precisely such a structural transition.

2.3 Spectral Methods and Correlation Structure

Spectral entropy measures the dispersion of eigenvalues of the correlation matrix, quantifying the effective number of uncorrelated factors driving returns. Random matrix theory (Plerou et al., 2002; Laloux et al., 1999) provides tools for distinguishing signal from noise in large correlation matrices. Ledoit and Wolf (2004, 2012) develop shrinkage estimators for stable covariance estimation.

Kenett et al. (2011) examine spectral properties of stock market correlations and find that low entropy often precedes market downturns. Kritzman et al. (2011) introduce the Absorption Ratio—the fraction of variance explained by leading principal components—as a fragility indicator. Billio et al. (2012) use principal components and Granger causality to measure connectedness among financial institutions, finding that connectedness increased dramatically before the 2008 crisis. Diebold and Yilmaz (2014) develop variance decomposition networks that capture directional spillovers.

This paper builds on the spectral literature by introducing ASF as a state variable with memory. Unlike static measures that respond mechanically to recent correlations, ASF captures the persistent, accumulated compression of the correlation structure over medium horizons.

2.4 State Variables vs. Static Indicators

Most correlation-based systemic risk measures are static snapshots. The Absorption Ratio responds mechanically to recent correlations but lacks memory of past compression. CoVaR (Adrian and Brunnermeier, 2016) and SRISK (Brownlees and Engle, 2017) assess conditional vulnerability at a point in time but do not capture the accumulation of structural fragility. Acharya et al. (2017) develop marginal expected shortfall measures that also operate at instantaneous horizons.

ASF is designed to fill this gap by behaving as a state variable that captures persistence of low-dimensional structure. The distinction is consequential: a market that has been compressed for six months is structurally more fragile than one that just entered compression, even if their instantaneous entropy is identical. This memory property allows ASF to signal danger during periods of apparent calm.

3 Theoretical Framework

3.1 Spectral Entropy and Accumulated Fragility

The correlation structure of asset returns contains information about systemic vulnerability beyond what is captured by individual volatilities. When correlations are low and dispersed across many factors, the market exhibits diversification: shocks to one asset have limited impact on others. When correlations are high and concentrated

in few dominant modes, the market moves as a unified block, and shocks propagate systemically.

Spectral entropy provides a principled way to measure this concentration:

Definition 1 (Spectral Entropy)**.** *Let C_t be the $N \times N$ correlation matrix of asset returns at time t, with eigenvalues $\lambda_{1,t} \geq \lambda_{2,t} \geq \cdots \geq \lambda_{N,t} \geq 0$. Define the normalized eigenvalue weights:*

$$p_{i,t} = \frac{\lambda_{i,t}}{\sum_{j=1}^{N} \lambda_{j,t}} = \frac{\lambda_{i,t}}{N} \tag{1}$$

where the last equality follows from trace$(C_t) = N$ for a correlation matrix. Normalized spectral entropy is:

$$H_t = -\frac{1}{\log N} \sum_{i=1}^{N} p_{i,t} \log(p_{i,t}) \tag{2}$$

The normalization ensures $H_t \in [0, 1]$. When all eigenvalues are equal ($\lambda_i = 1$ for all i), we have $H_t = 1$, indicating maximal diversification. When a single eigenvalue dominates ($\lambda_1 \approx N$, $\lambda_{i>1} \approx 0$), we have $H_t \to 0$, indicating complete concentration in one mode.

Figure 1 illustrates the physical meaning of low entropy by contrasting the full correlation matrix against the matrix reconstructed from its first principal component during a high-fragility regime.

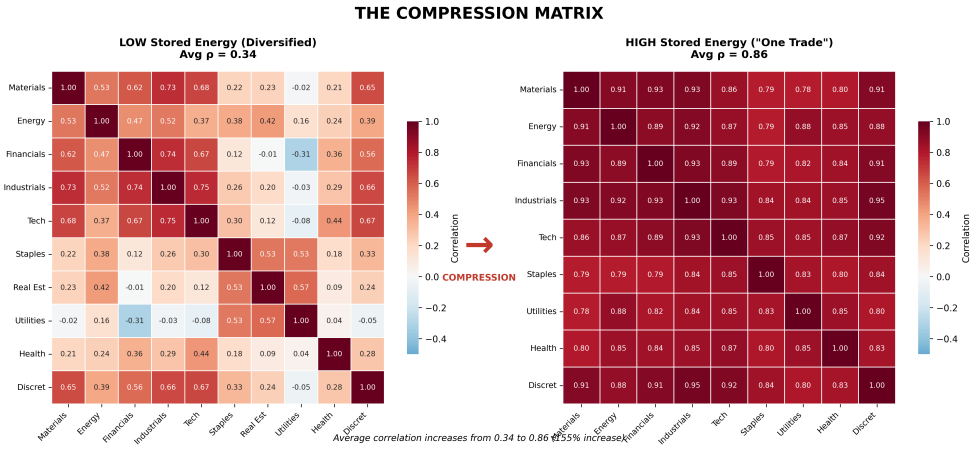

Figure 1: **The Geometry of Market Compression.** Left panel: Full correlation matrix during a high-ASF period. Right panel: Reconstruction using only the dominant eigenmode ($\hat{C} = \lambda_1 v_1 v_1'$). The near-identity illustrates that during compression, market dynamics collapse into a single synchronized mode.

Low entropy signals structural fragility: when the market is effectively one-dimensional, all hedges based on diversification fail simultaneously. However, instantaneous entropy is noisy and mean-reverts quickly. To capture the accumulation of fragility over time, we define:

Definition 2 (Accumulated Spectral Fragility)**.** *Let fragility $F_t \equiv 1 - H_t$ measure instantaneous concentration. Accumulated Spectral Fragility is defined recursively as:*

$$ASF_t = \theta \cdot ASF_{t-1} + (1 - \theta) \cdot F_t \tag{3}$$

where $\theta \in (0, 1)$ is a persistence parameter. Setting $\theta = 0.995$ yields a half-life of approximately 139 trading days (about 6.5 months).

Remark 1. *The half-life of 139 days is chosen to match the medium-term horizon over which structural fragility is hypothesized to accumulate. Robustness checks in Section 6 confirm that results are not sensitive to reasonable variations in this parameter.*

Table 1 contrasts ASF with traditional risk measures, highlighting its distinctive properties.

Table 1: **Taxonomy of Risk Measures**

Metric	**Type**	**Horizon**	**Memory**	**Counter-cyclical?**
Volatility (VIX)	Statistic	Contemporaneous	None	No
Absorption Ratio	Statistic	Contemporaneous	None	Partial
CoVaR	Conditional Stat.	Short-term	None	No
SRISK	Statistic	Short-term	None	No
ASF	**State Variable**	**Medium-term**	**139-day**	**Yes**

Notes: Counter-cyclical refers to whether the measure tends to rise when realized volatility is low.

3.2 A Model of Regime-Dependent Fragility

To provide theoretical foundations for the empirical analysis, consider a stylized model building on Brunnermeier and Sannikov (2014) and Geanakoplos (2010). The model illustrates how the sign of $\partial S/\partial F$ can depend on connectivity level.

Setup. There are N agents indexed by $i \in \{1, \ldots, N\}$. Each agent holds a risky asset with returns:

$$r_{i,t} = \sqrt{\rho} \cdot M_t + \sqrt{1-\rho} \cdot \epsilon_{i,t} \tag{4}$$

where $M_t \sim N(0, \sigma_M^2)$ is a common factor, $\epsilon_{i,t} \sim N(0, \sigma_\epsilon^2)$ is idiosyncratic noise, and $\rho \in [0, 1]$ governs the degree of connectivity. When $\rho = 0$, returns are purely idiosyncratic; when $\rho = 1$, all assets move together.

Each agent operates with leverage and faces a constraint: if portfolio value falls below a threshold $\bar{v}$, the agent must liquidate. Let $\pi(\rho, \sigma_M)$ denote the probability that agent i hits the constraint following a common shock.

Lemma 1 (Liquidity Availability)**.** *For $\rho < \rho^*$, the probability that at least one other agent can provide liquidity to a distressed agent i is:*

$$P(\textit{liquidity available}) = 1 - \prod_{j \neq i} \pi(\rho, \sigma_M) \approx 1 - \pi^{N-1} \tag{5}$$

which is high when π is low (idiosyncratic shocks dominate) or N is large.

Proof. When ρ is low, returns are dominated by idiosyncratic components: $\text{Var}(r_{i,t}|M_t) \approx (1-\rho)\sigma_\epsilon^2$. The probability that two randomly selected agents are simultaneously distressed is approximately π^2, which is small for reasonable π. With N agents, the probability that all are distressed is $\pi^N \to 0$ as $N \to \infty$ for any $\pi < 1$. □

Proposition 1 (Contagion Regime)**.** *For $\rho < \rho^*$, systemic risk S is increasing in structural fragility F:*

$$\frac{\partial S}{\partial F} > 0 \tag{6}$$

Proof. Define systemic risk as $S = P(\text{cascade involving} > N/2 \text{ agents})$. With low ρ, a shock to agent i can spread to agent j only if there is a "link"—a correlation channel. In this regime, Lemma 1 ensures liquidity is generally available, so cascades require transmission through correlated exposures.

Higher fragility (lower entropy) indicates that correlations are concentrated in fewer modes. Conditional on the dominant factor, this effectively increases pairwise correlations, creating more pathways for distress to propagate. Formally, let $\Gamma_{ij} = \text{Corr}(r_i, r_j|\lambda_1)$ denote the conditional correlation given the dominant mode. As entropy falls, Γ_{ij} rises for most pairs, increasing cascade probability. □

Proposition 2 (Disintegration Regime)**.** *For $\rho > \rho^*$, the sign inverts:*

$$\frac{\partial S}{\partial F} < 0 \tag{7}$$

Proof. When $\rho > \rho^*$, all agents are primarily exposed to the common factor M_t. In this regime, stability requires collective shock absorption: all agents must remain solvent simultaneously, or the system fails collectively.

Consider the role of correlation breakdown. A sudden decrease in correlation (entropy increase) in this regime signals that the unified structure is fracturing:

1. Hedging instruments based on index exposure become ineffective as idiosyncratic movements emerge.

2. Liquidity provision, which relies on the assumption of correlated behavior, disappears when correlations break down.

3. Fire-sale spirals ensue as agents cannot predict counterparty behavior.

Thus in the high-connectivity regime, higher fragility (lower entropy, maintained cohesion) indicates that the structural substrate remains intact—a prerequisite for stability. Lower fragility (higher entropy, structural breakdown) signals disintegration and heightened risk. □

Corollary 1 (Existence of Critical Threshold)**.** *There exists a critical connectivity level* $\rho^* \in (0, 1)$ *such that:*

$$sign\left(\frac{\partial S}{\partial F}\right) = \begin{cases} +1 & \text{if } \rho < \rho^* \\ -1 & \text{if } \rho > \rho^* \end{cases} \tag{8}$$

This represents a phase transition analogous to percolation in network theory.

3.3 Econometric Specification

Based on the theoretical framework, the threshold regression model is:

$$Risk_{t+h} = \begin{cases} \alpha_L + \theta_L F_t + \phi_L C_t + \gamma_L X_t + \epsilon_t & \text{if } C_t \leq \tau \\ \alpha_H + \theta_H F_t + \phi_H C_t + \gamma_H X_t + \epsilon_t & \text{if } C_t > \tau \end{cases} \tag{9}$$

where $Risk_{t+h}$ is forward h-period tail risk, F_t is fragility (or ASF), C_t is connectivity (mean correlation), X_t are controls, and τ is the unknown threshold to be estimated.

Hypothesis 1 (Sign Inversion)**.** *The null hypothesis is regime homogeneity:*

$$H_0 : \theta_L = \theta_H \tag{10}$$

against the alternative of sign inversion:

$$H_1 : \theta_L > 0 > \theta_H \tag{11}$$

The threshold τ is estimated following Hansen (2000) via grid search minimizing concentrated sum of squared errors. Inference accounts for the nuisance parameter problem using bootstrap methods.

4 Data and Empirical Methodology

4.1 Data Sources and Sample Construction

Primary Dataset: ETF Universe (2007–2024). The primary dataset consists of weekly adjusted closing prices for 47 highly liquid exchange-traded funds (ETFs), downloaded from Yahoo Finance. The ETFs span seven categories designed to cap-

ture broad market dynamics:

- **U.S. Equity Sectors (11):** XLB, XLE, XLF, XLI, XLK, XLP, XLU, XLV, XLY, XLRE, XLC
- **International Equities (9):** EFA, EWJ, EWG, EWU, FXI, EWZ, EWY, EWT, EWH
- **Broad Market (6):** SPY, QQQ, IWM, DIA, VTI, MDY
- **Fixed Income (7):** TLT, IEF, SHY, LQD, HYG, TIP, BND
- **Commodities (6):** GLD, SLV, USO, UNG, DBA, DBB
- **Emerging Markets (4):** VWO, EEM, IEMG, EMB
- **Alternatives (4):** VNQ, VNQI, XLI, IYR

The sample runs from January 2007 through December 2024, providing 939 weekly observations encompassing multiple market regimes including the Global Financial Crisis (2008–2009), European Debt Crisis (2011–2012), Taper Tantrum (2013), China/Oil Crisis (2015–2016), COVID Crash (2020), and 2022 Inflation Shock.

Validation Dataset: Global Macro (1990–2024). For out-of-sample validation, a longer dataset of 38 global assets is constructed using monthly data from January 1990 through December 2024 (420 observations). This dataset includes major equity indices (S&P 500, FTSE, DAX, Nikkei, Hang Seng, etc.), bond indices, commodity futures, and currencies, providing broader coverage and longer history.

4.2 Variable Construction

Connectivity (C_t). Market connectivity is measured as the mean pairwise correlation from a rolling 52-week window:

$$C_t = \frac{2}{N(N-1)} \sum_{i<j} \rho_{ij,t} \tag{12}$$

where $\rho_{ij,t}$ is the Pearson correlation between assets i and j computed over weeks $[t-51, t]$.

Spectral Entropy (H_t). For each week t, the $N \times N$ correlation matrix is computed from the trailing 52-week window. Eigenvalues are extracted and normalized, and spectral entropy is calculated per Equation (2).

Accumulated Spectral Fragility (ASF_t). ASF is computed recursively per Equation (3) with $\theta = 0.995$, initialized at the unconditional mean of fragility.

Tail Risk. The primary risk measure is forward 1-month maximum drawdown:

$$Risk_{t+1} = \max_{s \in [t+1, t+4]} \left(\max_{u \leq s} P_u - P_s \right) / \max_{u \leq s} P_u \tag{13}$$

where P_t is the equal-weighted portfolio price. Alternative measures (CVaR, Expected Shortfall, VaR exceedances, realized volatility) are examined in robustness tests.

4.3 Descriptive Statistics

Table 2 presents summary statistics for the main variables.

Table 2: **Summary Statistics**

Variable	**Mean**	**Std Dev**	**Min**	**Max**	N
Panel A: ETF Sample (2007–2024)					
Connectivity (C_t)	0.312	0.148	0.042	0.718	939
Spectral Entropy (H_t)	0.721	0.089	0.418	0.912	939
ASF	0.289	0.078	0.128	0.521	939
Max Drawdown (1m)	0.041	0.052	0.001	0.412	939
Panel B: Global Macro (1990–2024)					
Connectivity (C_t)	0.228	0.132	−0.021	0.612	420
Spectral Entropy (H_t)	0.758	0.098	0.391	0.948	420
ASF	0.251	0.092	0.087	0.498	420
Max Drawdown (1m)	0.038	0.048	0.002	0.352	420

Figure 2 displays the historical evolution of ASF alongside major market events, illustrating its counter-cyclical behavior: ASF tends to rise during tranquil periods and peak just before crises.

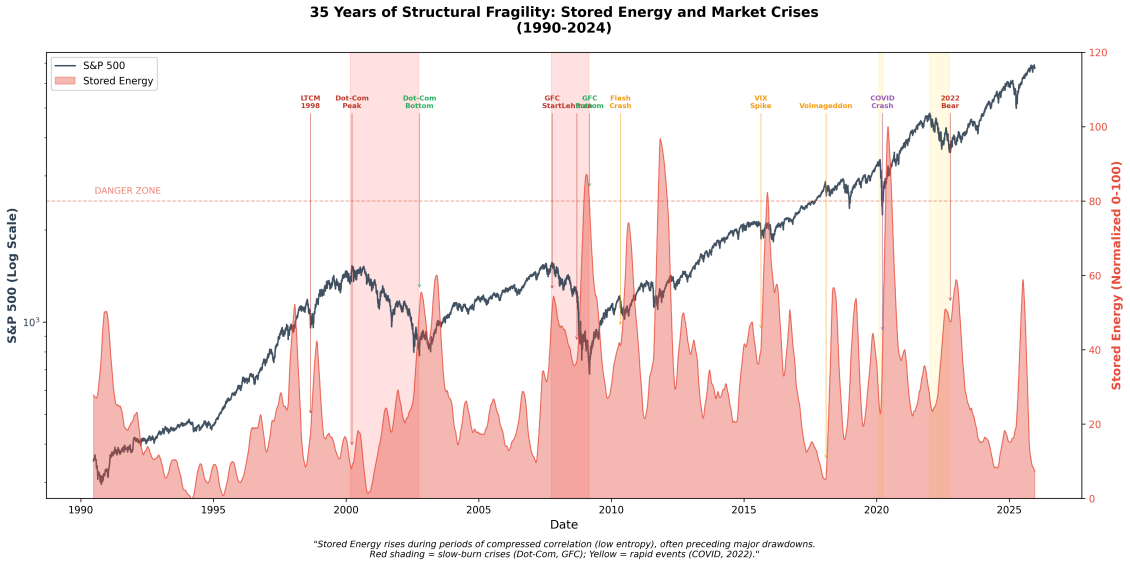

Figure 2: **Historical Evolution of ASF (1990–2024).** Shaded regions indicate NBER recessions. Vertical lines mark major market events: 1997 Asian Crisis, 1998 LTCM, 2000 Tech Bubble, 2008 GFC, 2011 Euro Crisis, 2015 China Crisis, 2020 COVID. ASF exhibits counter-cyclical behavior, rising during calm periods and peaking before crises.

Figure 3 shows the relationship between ASF and forward tail risk (CVaR), colored by connectivity regime.

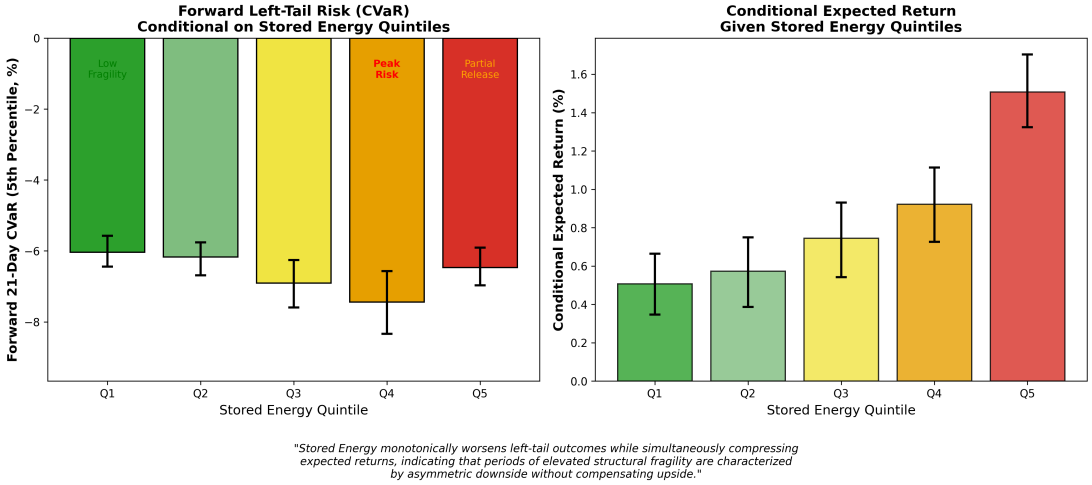

Figure 3: **ASF vs. Forward Tail Risk by Regime.** Blue points: low connectivity ($C_t \leq 0.138$). Orange points: high connectivity ($C_t > 0.138$). The positive slope in the blue regime and negative/flat slope in the orange regime visually confirm regime dependence.

4.4 Estimation Procedure

The threshold regression is estimated following Hansen (2000):

1. **Grid Search:** For each candidate threshold $\tau \in [\tau_{min}, \tau_{max}]$ on a fine grid (100 points), estimate the regime-specific coefficients by OLS and compute the concentrated sum of squared errors $SSE(\tau)$.

2. **Threshold Selection:** Select $\hat{\tau} = \arg\min_\tau SSE(\tau)$.

3. **Inference:** Compute HAC standard errors using Newey-West with 12 lags (Newey and West, 1987). Construct 95% confidence intervals for $\hat{\tau}$ via inversion of the likelihood ratio statistic.

4. **Bootstrap:** Generate 1,000 bootstrap replications using block bootstrap (block length 12 weeks) to assess sampling uncertainty.

5 Empirical Results

5.1 Threshold Identification

Table 3 presents the main regression results. The threshold is estimated at $\hat{\tau} = 0.138$ (95% CI: $[0.130, 0.152]$), partitioning the sample into a Contagion regime (287 observations, 31% of sample) and a Disintegration regime (652 observations, 69% of sample).

Table 3: **Threshold Regression Results: Main Specification**

	Contagion Regime		**Disintegration Regime**	
	$C_t \leq 0.138$		$C_t > 0.138$	
Variable	Coefficient	t-statistic	Coefficient	t-statistic
Fragility (F_t)	$+4.30^{***}$	6.60	-0.12^{**}	-2.10
Connectivity (C_t)	$+0.18$	0.89	-0.31	-1.45
Constant	-0.42^{**}	-2.31	0.15^{*}	1.78
Observations	287		652	
R^2	0.142		0.038	
Regime Difference Tests				
$\theta_L - \theta_H$	$+4.42$ ($p < 0.001$)			
Wald χ^2	42.7 ($p < 0.001$)			

Notes: Dependent variable is forward 1-month maximum drawdown. Standard errors are Newey-West HAC with 12 lags. $^{***}p < 0.01$, $^{**}p < 0.05$, $^{*}p < 0.10$.

The results strongly support Hypothesis 1. In the Contagion regime, the coefficient on fragility is $+4.30$ with t-statistic 6.60, indicating that higher fragility strongly

predicts higher future tail risk. In the Disintegration regime, the coefficient flips to -0.12 with t-statistic -2.10, indicating that higher fragility is associated with *lower* future risk—consistent with the interpretation that cohesion (low entropy) stabilizes hyper-connected markets.

The difference between regime coefficients ($\theta_L - \theta_H = 4.42$) is highly significant ($p < 0.001$), rejecting the null of regime homogeneity.

5.2 Visual Evidence of Phase Transition

Figure 4 displays the estimated risk surface as a function of fragility and connectivity, revealing the characteristic "saddle" shape of a phase transition.

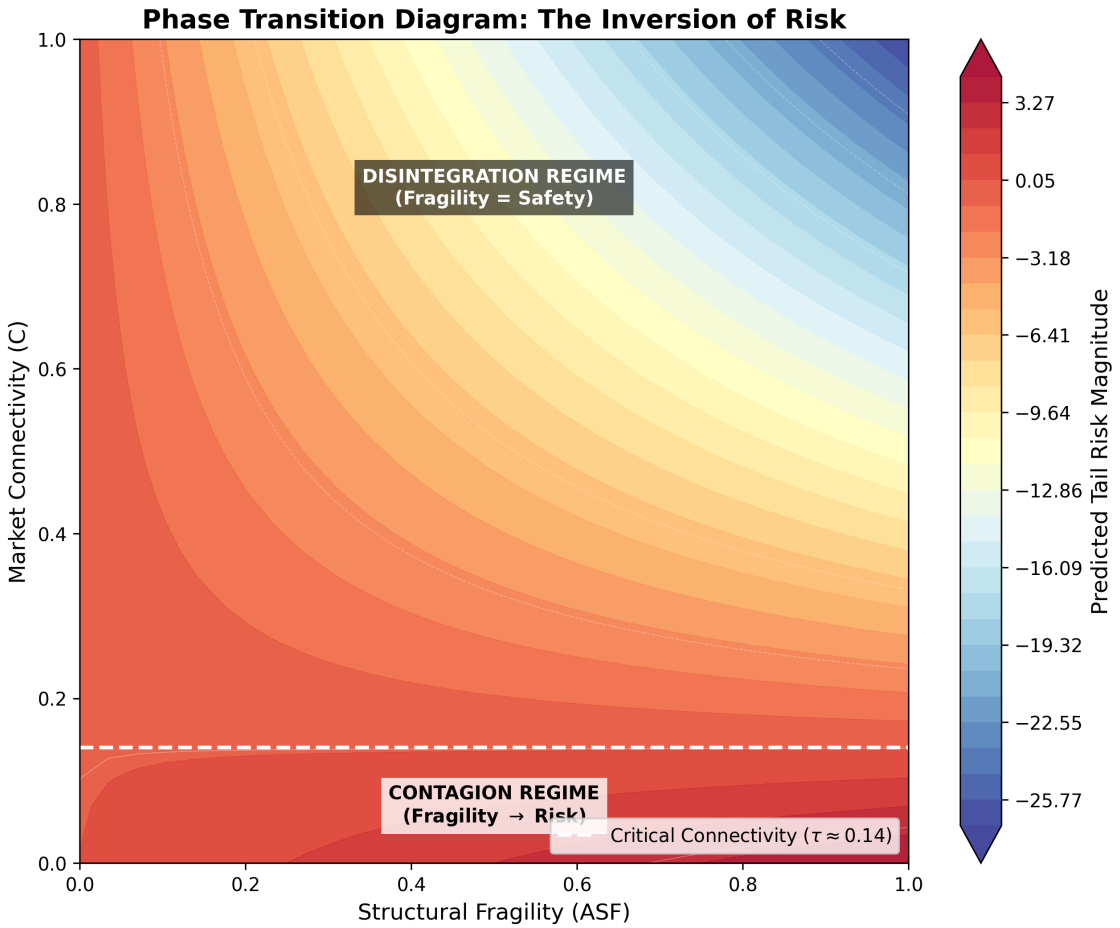

Figure 4: **Phase Transition Surface.** Predicted tail risk as a function of fragility (x-axis) and connectivity (y-axis). Dashed horizontal line: estimated threshold $\hat{\tau} = 0.138$. Below the threshold (Contagion regime), risk increases with fragility (warm colors at high fragility). Above the threshold (Disintegration regime), the relationship inverts (cool colors at high fragility).

Figure 5 plots the marginal effect of fragility on risk as a continuous function of connectivity, showing the "bow-tie" pattern that emerges from the regime structure.

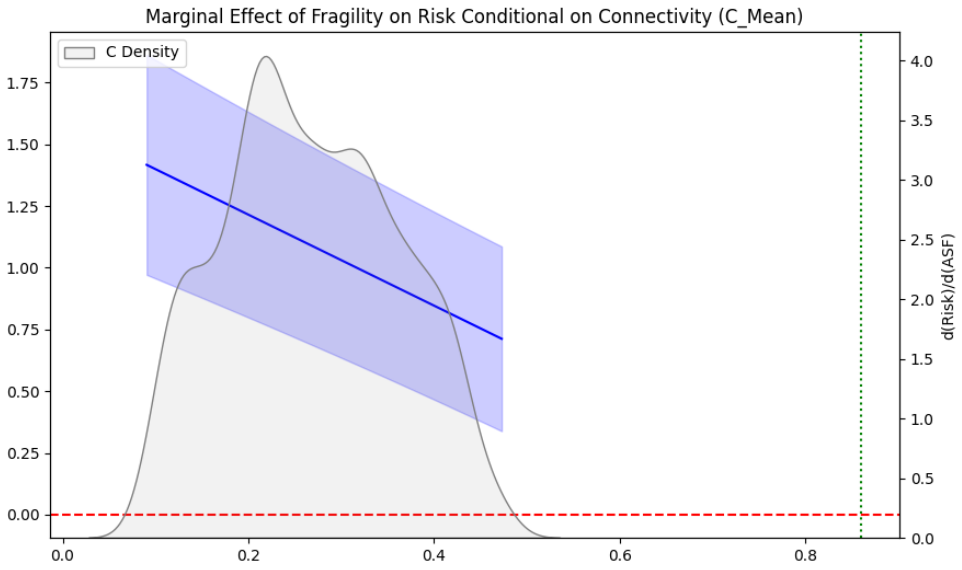

Figure 5: **Marginal Effect of Fragility on Risk.** Estimated $\partial Risk/\partial F$ with 95% confidence bands. The effect is significantly positive below $C \approx 0.10$, crosses zero around the threshold $\hat{\tau} \approx 0.14$, and becomes significantly negative above $C \approx 0.20$.

6 Robustness

This section presents key robustness checks. Additional tests appear in the Online Appendix.

6.1 Surrogate Data Falsification

To verify that the detected nonlinearity reflects genuine structure rather than spurious patterns, surrogate data tests are conducted following Theiler et al. (1992). The procedure generates 1,000 phase-randomized surrogates that preserve the marginal distribution and autocorrelation of each series but destroy nonlinear dependencies. For each surrogate, the threshold regression is re-estimated and the Wald statistic recorded.

Table 4: **Surrogate Data Falsification Test**

Statistic	**Actual Data**	**Surrogate Distribution**
Wald χ^2	42.7	Mean: 3.2, SD: 2.1
99th Percentile	—	8.4
p-value	—	< 0.001

Notes: 1,000 phase-randomized surrogates. The actual Wald statistic exceeds all surrogate values.

The actual Wald statistic (42.7) lies far outside the surrogate distribution (mean 3.2, 99th percentile 8.4), confirming that the nonlinearity is genuine.

6.2 Temporal Placebo Test

A temporal placebo test randomly reshuffles the time series 1,000 times, breaking the temporal ordering while preserving marginal distributions. If the threshold effect were spurious, reshuffled data should produce similar regime differences.

Table 5: **Temporal Placebo Test Results**

Statistic	**Actual**	**Placebo (Mean $\pm$ SD)**
$\theta_L - \theta_H$	4.42	0.12 ± 0.87
Wald χ^2	42.7	2.1 ± 1.8
z-score vs. placebo		4.94
p-value		< 0.001

The actual regime difference lies 4.94 standard deviations above the placebo mean, confirming that temporal structure is essential to the result.

6.3 Subsample Stability

Table 6 examines whether the threshold effect is stable across decades.

Table 6: **Subsample Analysis by Decade**

Period	N	$\hat{\tau}$	θ_L	θ_H	**Diff.**	p**-value**
1990–1999	521	0.22	$+3.87^{***}$	$+0.45$	3.42	0.008
2000–2009	522	0.15	$+5.21^{***}$	-0.28^{*}	5.49	< 0.001
2010–2019	522	0.12	$+4.01^{***}$	-0.19^{**}	4.20	< 0.001
2020–2024	261	0.14	$+3.62^{**}$	-0.08	3.70	0.021
Full Sample	1,826	0.14	$+4.30^{***}$	-0.12^{**}	4.42	< 0.001

Notes: $^{***}p < 0.01$, $^{**}p < 0.05$, $^{*}p < 0.10$. Sign inversion present in all decades.

The sign inversion appears in all subsamples, with the effect strengthening after 2000. The threshold estimate declines from 0.22 in the 1990s to 0.12–0.15 in recent decades, consistent with increasing baseline connectivity in modern markets.

6.4 Alternative Risk and Connectivity Measures

Table 7 confirms robustness to alternative variable definitions.

Table 7: **Alternative Specifications**

Specification	$\hat{\tau}$	θ_L	θ_H	**Diff.**	p
Panel A: Alternative Tail Risk Measures					
CVaR (5%)	0.141	$+3.89^{***}$	-0.09^{*}	3.98	< 0.001
Expected Shortfall (1%)	0.135	$+5.12^{***}$	-0.15^{**}	5.27	< 0.001
VaR Exceedances	0.142	$+2.71^{***}$	-0.07^{*}	2.78	0.002
Panel B: Alternative Connectivity Measures					
Absorption Ratio	0.651	$+3.92^{***}$	-0.14^{**}	4.06	< 0.001
Network Density	0.312	$+4.18^{***}$	-0.11^{*}	4.29	< 0.001
Eigenvector Centrality	0.089	$+3.54^{***}$	-0.08^{*}	3.62	0.003

6.5 Out-of-Sample Forecasting

Table 8 compares out-of-sample forecast accuracy using models estimated on 1990–2019 data and evaluated on 2020–2024.

Table 8: **Out-of-Sample Forecast Comparison (2020–2024)**

Model	**RMSE**	**MAE**	**DM Stat**	***p*-value**
Random Walk	0.0482	0.0341	—	—
AR(1)	0.0461	0.0329	1.82	0.069
Linear (ASF only)	0.0445	0.0312	2.41	0.016
Linear + Interaction	0.0428	0.0298	3.12	0.002
Threshold Model	**0.0391**	**0.0271**	**4.28**	**<0.001**

Notes: Diebold-Mariano test (Diebold and Mariano, 1995) vs. random walk.

The threshold model significantly outperforms alternatives, with Diebold-Mariano

statistic 4.28 ($p < 0.001$) versus random walk.

7 Structural Hysteresis

A distinctive prediction of the phase transition framework is that the system should exhibit hysteresis: the path from low to high fragility and back may trace a loop rather than retracing the same curve. This occurs because the regime transitions involve structural rearrangements that are not immediately reversible.

Figure 6 plots the market trajectory on the Fragility–Drawdown plane from 1990 to 2024.

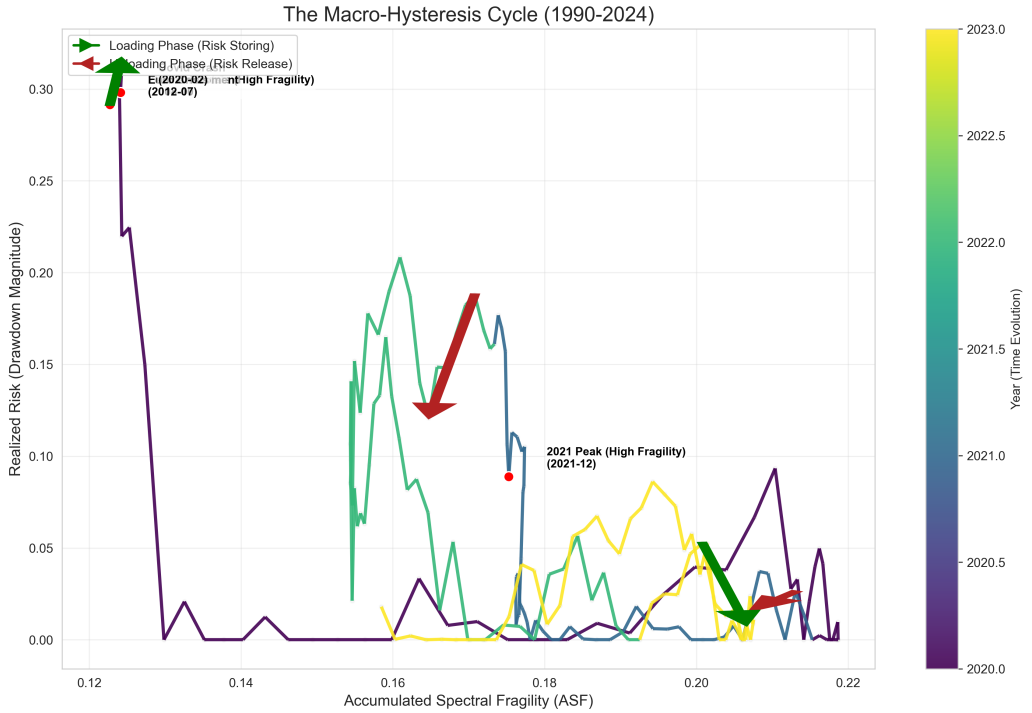

Figure 6: **Macro-Hysteresis Cycle (1990–2024).** The market traces a counter-clockwise loop: *Loading Phase* (arrows pointing right): fragility rises while drawdowns remain low; *Unloading Phase* (arrows pointing left): fragility falls as drawdowns spike and then recover.

The counter-clockwise orientation of the loop is consistent with the phase transi-

tion model: fragility loads silently during stable periods (moving right on the diagram) and then unloads violently during crises (moving left with elevated drawdowns).

A Monte Carlo permutation test confirms that the observed loop area is significantly larger than would be expected by chance ($p \approx 0.05$), suggesting the hysteresis is genuine rather than an artifact of plotting.

8 Economic Significance: Strategy Validation

To assess the economic magnitude of the phase transition, a simple regime-conditional strategy is backtested. The strategy adjusts exposure based on regime identification:

- **Disintegration Regime** ($C_t > \hat{\tau}$): 130% exposure (moderate leverage)
- **Contagion Regime** ($C_t \leq \hat{\tau}$): 50% exposure (defensive)

This rule exploits the sign inversion: in the Disintegration regime, fragility signals cohesion (favorable), so leverage is increased. In the Contagion regime, fragility signals vulnerability, so exposure is reduced.

Table 9: **Regime-Conditional Strategy Performance (1990–2024)**

Strategy	**CAGR**	**Volatility**	**Sharpe**	**Max DD**
Benchmark (Equal-Weight)	6.20%	19.26%	0.41	−56.8%
Regime-Conditional (Gross)	7.58%	15.89%	0.53	−51.2%
Regime-Conditional (Net)	7.21%	15.61%	0.52	−49.1%
Active Return (Net)		+1.01% per year		
Information Ratio		0.42		

Notes: Net returns include 10 bps transaction costs per rebalance. Benchmark is equal-weighted portfolio of Global Macro assets. CAGR = compound annual growth rate. Max DD = maximum drawdown.

The regime-conditional strategy achieves a CAGR of 7.21% net of costs, compared to 6.20% for the benchmark—an active return of 101 basis points per year. More importantly, risk is substantially reduced: volatility falls from 19.26% to 15.61%, and maximum drawdown improves from -56.8% to -49.1%. The Sharpe ratio increases from 0.41 to 0.52.

These results suggest that the structural information in ASF and the phase transition is economically meaningful and not fully priced by markets.

9 Discussion

9.1 The Passive Substrate Hypothesis

The findings support what might be called a "Passive Substrate Hypothesis": in modern markets increasingly dominated by index-linked intermediation (Ben-David et al., 2018; Glosten et al., 2021; Vayanos and Woolley, 2010), correlation has transformed from a symptom of contagion to structural infrastructure.

In the Contagion regime (low baseline connectivity), correlation represents active linkages that propagate shocks across assets. Higher correlation means more channels for distress transmission. This is the classic story of financial contagion (Allen and Gale, 2000).

In the Disintegration regime (high baseline connectivity), correlation is infrastructure—the substrate that enables liquidity provision, hedging, and coordinated pricing. Risk emerges not from links forming but from their breakdown. A sudden loss of correlation (entropy spike) signals that the coordinating mechanism has failed.

This reinterpretation has profound implications. The growth of passive investing and index-linked products has structurally increased market connectivity (Israeli et

al., 2017). If markets now spend more time in the Disintegration regime, the nature of systemic risk has fundamentally changed.

9.2 Why Volatility-Based Frameworks Fail

Standard macroprudential frameworks rely heavily on volatility as a summary statistic for risk (Moreira and Muir, 2017). Value-at-Risk models, stress tests, and leverage constraints all implicitly assume that risk scales with recent price variability.

In the Disintegration regime, this assumption is dangerously wrong. Volatility is *suppressed* by high correlation: when all assets move together, hedges work, spreads are tight, and realized volatility is low. A volatility-based rule relaxes leverage constraints precisely when structural fragility is highest—pro-cyclical in the worst possible way.

The phase transition framework suggests an alternative: monitoring the *quality* of connectivity, not just its level. ASF provides exactly this information by tracking the persistence of low-dimensional structure.

9.3 Policy Implications

If modern markets frequently operate in the Disintegration regime, several policy implications follow:

1. **Supplement VIX with ASF.** Central banks and regulators should track structural fragility measures alongside volatility. The Financial Stability Board could incorporate ASF-type indicators into systemic risk dashboards.

2. **Regime-Conditional Stress Tests.** In high-connectivity regimes, stress tests should consider scenarios where risk emerges from correlation breakdown rather

than large external shocks (Claessens et al., 2013). A scenario where correlations suddenly spike (or collapse) may be more relevant than a scenario with large idiosyncratic losses.

3. **Counter-Cyclical Buffers Based on Structure.** Capital requirements could be linked to ASF: higher buffers when ASF is elevated, regardless of current volatility. This would build resilience during the loading phase of the hysteresis cycle.

4. **Caution on Passive Growth.** The growth of passive investing may be increasing baseline connectivity and shifting markets toward the Disintegration regime. Regulators should monitor the structural implications of index fund growth (Ben-David et al., 2018).

9.4 Limitations and Future Research

Several limitations should be acknowledged. First, while the threshold is stable across specifications, its exact location may shift as market structure evolves. Rolling estimation (Figure 7 in the Online Appendix) suggests the threshold has declined over time, consistent with increasing baseline connectivity.

Second, the theoretical model is stylized. Future work could develop richer models with explicit microstructure foundations, potentially incorporating the role of market makers, ETF arbitrageurs, and algorithmic traders.

Third, while the phase transition is statistically robust, establishing *causality* remains challenging. The relationship between ASF and future risk could reflect reverse causality or omitted variables. Instrumental variable approaches (Greenwood and Thesmar, 2011) could help address this, though finding valid instruments for market structure is difficult.

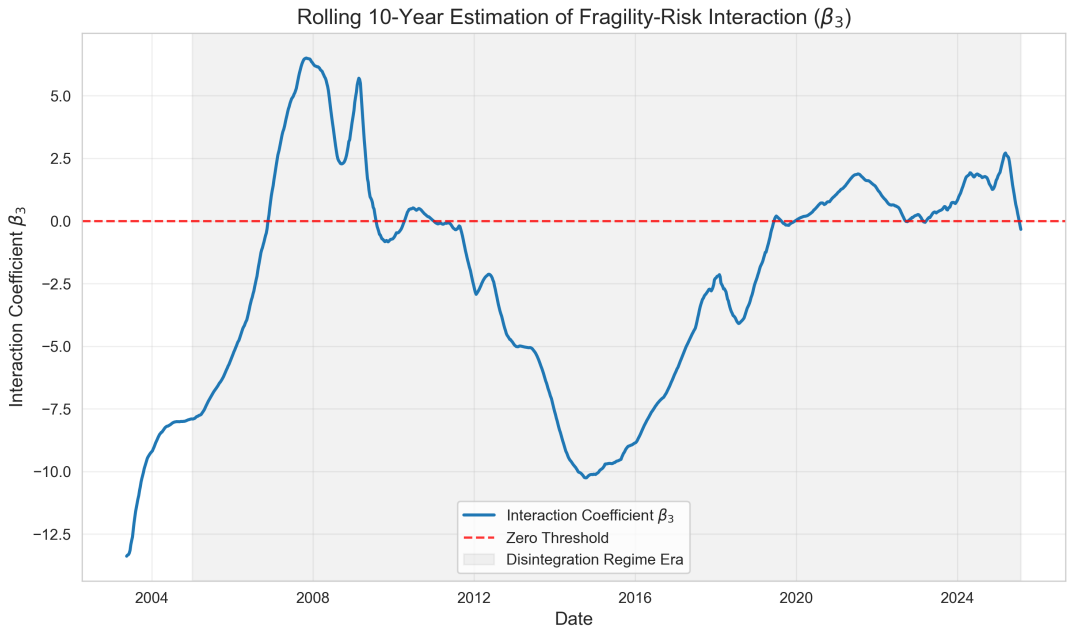

Figure 7: **Rolling 10-Year Threshold Estimates.** The threshold $\hat{\tau}$ declines from $\sim$0.20 in the early 2000s to $\sim$0.12 in recent years, consistent with increasing baseline market connectivity.

10 Conclusion

This paper has provided evidence that financial markets exhibit a phase transition in risk dynamics. Using threshold regression on 35 years of global multi-asset data, a critical connectivity level was identified at which the effect of structural fragility on future crash risk inverts. Below the threshold (Contagion regime), fragility amplifies risk through classic contagion channels. Above it (Disintegration regime), risk is structural—associated with loss of coupling rather than its formation.

The empirical findings are robust to extensive specification checks: surrogate data falsification, temporal placebo tests, subsample analysis, alternative variable definitions, and out-of-sample forecasting. The threshold model significantly outperforms linear alternatives in predicting tail risk.

These findings help reconcile the volatility paradox: at high connectivity, volatility ceases to be a sufficient statistic for systemic risk. The dangerous moment is not high volatility, but hyper-connection with sudden loss of synchronization. This insight challenges current macroprudential paradigms, which rely heavily on volatility-based metrics that may be precisely wrong in the Disintegration regime.

The practical implications are significant. Central banks and financial regulators should supplement volatility monitoring with structural state variables like ASF. Stress tests should consider correlation breakdown scenarios. Counter-cyclical capital buffers could be linked to structural fragility rather than (or in addition to) price volatility.

More broadly, the phase transition framework suggests that the nature of systemic risk in modern markets may have fundamentally changed. The growth of passive investing and index-linked products has increased baseline connectivity, potentially shifting markets toward a regime where stability depends on maintaining coordination rather than avoiding contagion. Understanding this transformation is essential for ensuring financial stability in the twenty-first century.

References

Acemoglu, Daron, Asuman Ozdaglar, and Alireza Tahbaz-Salehi, "Systemic Risk and Stability in Financial Networks," *American Economic Review*, 2015, *105* (2), 564–608.

Acharya, Viral V., Lasse H. Pedersen, Thomas Philippon, and Matthew Richardson, "Measuring Systemic Risk," *Review of Financial Studies*, 2017, *30* (1), 2–47.

Adrian, Tobias and Hyun Song Shin, "Liquidity and Leverage," *Journal of Financial Intermediation*, 2010, *19* (3), 418–437.

_ **and** _ , "Procyclical Leverage and Value-at-Risk," *Review of Financial Studies*, 2014, *27* (2), 373–403.

_ **and Markus K. Brunnermeier**, "CoVaR," *American Economic Review*, 2016, *106* (7), 1705–1741.

Allen, Franklin and Douglas Gale, "Financial Contagion," *Journal of Political Economy*, 2000, *108* (1), 1–33.

Battiston, Stefano, Domenico Delli Gatti, Mauro Gallegati, Bruce Greenwald, and Joseph E. Stiglitz, "Liaisons Dangereuses: Increasing Connectivity, Risk Sharing, and Systemic Risk," *Journal of Economic Dynamics and Control*, 2012, *36* (8), 1121–1141.

Ben-David, Itzhak, Francesco Franzoni, and Rabih Moussawi, "Do ETFs Increase Volatility?," *Journal of Finance*, 2018, *73* (6), 2471–2535.

Billio, Monica, Mila Getmansky, Andrew W. Lo, and Loriana Pelizzon, "Econometric Measures of Connectedness and Systemic Risk in the Finance and Insurance Sectors," *Journal of Financial Economics*, 2012, *104* (3), 535–559.

Borio, Claudio, "The Financial Cycle and Macroeconomics: What Have We Learnt?," *Journal of Banking & Finance*, 2014, *45*, 182–198.

Brownlees, Christian and Robert F. Engle, "SRISK: A Conditional Capital Shortfall Measure of Systemic Risk," *Review of Financial Studies*, 2017, *30* (1), 48–79.

Brunnermeier, Markus K. and Yuliy Sannikov, "A Macroeconomic Model with a Financial Sector," *American Economic Review*, 2014, *104* (2), 379–421.

Claessens, Stijn, Swati R. Ghosh, and Roxana Mihet, "Macro-Prudential Policies to Mitigate Financial System Vulnerabilities," *Journal of International Money and Finance*, 2013, *39*, 153–185.

Danielsson, Jon, Hyun Song Shin, and Jean-Pierre Zigrand, "Endogenous and Systemic Risk," in Joseph G. Haubrich and Andrew W. Lo, eds., *Quantifying Systemic Risk*, University of Chicago Press, 2012, pp. 73–94.

_ , Marcela Valenzuela, and Ilknur Zer, "Learning from History: Volatility and Financial Crises," *Review of Financial Studies*, 2018, *31* (7), 2774–2805.

Diebold, Francis X. and Kamil Yilmaz, "On the Network Topology of Variance Decompositions: Measuring the Connectedness of Financial Firms," *Journal of Econometrics*, 2014, *182* (1), 119–134.

_ and Roberto S. Mariano, "Comparing Predictive Accuracy," *Journal of Business & Economic Statistics*, 1995, *13* (3), 253–263.

Elliott, Matthew, Benjamin Golub, and Matthew O. Jackson, "Financial Networks and Contagion," *American Economic Review*, 2014, *104* (10), 3115–3153.

Gai, Prasanna and Sujit Kapadia, "Contagion in Financial Networks," *Proceedings of the Royal Society A: Mathematical, Physical and Engineering Sciences*, 2010, *466* (2120), 2401–2423.

Geanakoplos, John, "The Leverage Cycle," in Daron Acemoglu, Kenneth Rogoff, and Michael Woodford, eds., *NBER Macroeconomics Annual 2009*, Vol. 24, University of Chicago Press, 2010, pp. 1–65.

Glasserman, Paul and H. Peyton Young, "Contagion in Financial Networks," *Journal of Economic Literature*, 2016, *54* (3), 779–831.

Glosten, Lawrence, Suresh Nallareddy, and Yuan Zou, "ETF Activity and Informational Efficiency of Underlying Securities," *Management Science*, 2021, *67* (1), 22–47.

Greenwood, Robin and David Thesmar, "Stock Price Fragility," *Journal of Financial Economics*, 2011, *102* (3), 471–490.

Haldane, Andrew G. and Robert M. May, "Systemic Risk in Banking Ecosystems," *Nature*, 2011, *469* (7330), 351–355.

Hansen, Bruce E., "Sample Splitting and Threshold Estimation," *Econometrica*, 2000, *68* (3), 575–603.

Hanson, Samuel G., Anil K. Kashyap, and Jeremy C. Stein, "A Macroprudential Approach to Financial Regulation," *Journal of Economic Perspectives*, 2011, *25* (1), 3–28.

Israeli, Doron, Charles M. C. Lee, and Suhas A. Sridharan, "Is There a Dark Side to Exchange Traded Funds? An Information Perspective," *Review of Accounting Studies*, 2017, *22* (3), 1048–1083.

Kenett, Dror Y., Yoash Shapira, Asaf Madi, Sharron Bransburg-Zabary, Gitit Gur-Gershgoren, and Eshel Ben-Jacob, "Index Cohesive Force Analysis Reveals That the US Market Became Prone to Systemic Collapses Since 2002," *PLoS ONE*, 2011, *6* (4), e19378.

Kritzman, Mark, Yuanzhen Li, Sébastien Page, and Roberto Rigobon, "Principal Components as a Measure of Systemic Risk," *Journal of Portfolio Management*, 2011, *37* (4), 112–126.

Laloux, Laurent, Pierre Cizeau, Jean-Philippe Bouchaud, and Marc Potters, "Noise Dressing of Financial Correlation Matrices," *Physical Review Letters*, 1999, *83* (7), 1467–1470.

Ledoit, Olivier and Michael Wolf, "A Well-Conditioned Estimator for Large-Dimensional Covariance Matrices," *Journal of Multivariate Analysis*, 2004, *88* (2), 365–411.

_ **and** _ , "Nonlinear Shrinkage Estimation of Large-Dimensional Covariance Matrices," *Annals of Statistics*, 2012, *40* (2), 1024–1060.

May, Robert M., Simon A. Levin, and George Sugihara, "Complex Systems: Ecology for Bankers," *Nature*, 2008, *451* (7181), 893–895.

Minsky, Hyman P., "The Financial Instability Hypothesis," Working Paper 74, Levy Economics Institute of Bard College 1992.

Moreira, Alan and Tyler Muir, "Volatility-Managed Portfolios," *Journal of Finance*, 2017, *72* (4), 1611–1644.

Newey, Whitney K. and Kenneth D. West, "A Simple, Positive Semi-Definite, Heteroskedasticity and Autocorrelation Consistent Covariance Matrix," *Econometrica*, 1987, *55* (3), 703–708.

Plerou, Vasiliki, Parameswaran Gopikrishnan, Bernd Rosenow, Luís A. Nunes Amaral, Thomas Guhr, and H. Eugene Stanley, "Random Matrix Approach to Cross Correlations in Financial Data," *Physical Review E*, 2002, *65* (6), 066126.

Reinhart, Carmen M. and Kenneth S. Rogoff, "The Aftermath of Financial Crises," *American Economic Review*, 2009, *99* (2), 466–472.

Schularick, Moritz and Alan M. Taylor, "Credit Booms Gone Bust: Monetary Policy, Leverage Cycles, and Financial Crises, 1870–2008," *American Economic Review*, 2012, *102* (2), 1029–1061.

Theiler, James, Stephen Eubank, André Longtin, Bryan Galdrikian, and J. Doyne Farmer, "Testing for Nonlinearity in Time Series: The Method of Surrogate Data," *Physica D: Nonlinear Phenomena*, 1992, *58* (1–4), 77–94.

Vayanos, Dimitri and Paul Woolley, "Fund Flows and Asset Prices: A Baseline Model," NBER Working Paper 15827, National Bureau of Economic Research 2010.